Available online at www.sciencedirect.com
ScienceDirect
Geoderma 143 (2008) 206 – 215
GEODERMA
www.elsevier.com/locate/geoderma

Key soil and topographic properties to delineate potential management classes for precision agriculture in the European loess area

Udayakantha W.A. Vitharana [a,*], Marc Van Meirvenne [a], David Simpson [a], Liesbet Cockx [a], Josse De Baerdemaeker [b]

[a] Research Group Soil Spatial Inventory Techniques, Department of Soil Management and Soil Care, Ghent University, Coupure 653, 9000 Gent, Belgium
[b] Laboratory for Agricultural Machinery and Processing, K.U. Leuven, Kasteelpark Arenberg 30, 3001 Leuven, Belgium

Received 23 November 2006; received in revised form 5 September 2007; accepted 4 November 2007
Available online 3 December 2007

Abstract

Recent advances in on-the-go soil sensing, terrain modelling and yield mapping have made available large quantities of information about the within-field variability of soil and crop properties. But the selection of the key variables for an identification of management zones, required for precision agriculture, is not straightforward. To investigate a procedure for this selection, an 8 ha agricultural field in the Loess belt of Belgium was considered for this study. The available information consisted of: (i) top- and subsoil samples taken at 110 locations, on which soil properties: textural fractions, organic carbon (OC), $CaCO_3$ and pH were analysed, (ii) soil apparent electrical conductivity (EC_a) obtained through an electromagnetic induction based sensor, and (iii) wetness index, stream power index and steepest slope angle derived from a detailed digital elevation model (DEM). A principal component analysis, involving 12 soil and topographic properties and two EC_a variables, identified three components explaining 67.4% of the total variability. These three components were best represented by pH, EC_a that strongly associated with texture and OC. However, OC was closely related to some more readily obtainable topographic properties, and therefore elevation was preferred. A fuzzy *k*-means classification of these three variables produced four potential management classes. Three-year average standardized yield maps of grain and straw showed productivity differences across these classes, but mainly linked to their landscape position. In the loess area with complex soil-landscape interactions pH, EC_a and elevation can be considered as key properties to delineate potential management classes.

Keywords: Precision agriculture; Principal component analysis; Fuzzy *k*-means; EM38

1. Introduction

Soils derived from loess parent materials are recognized as among the most fertile of Europe. Consequently, they have been under intensive agriculture for centuries. A number of studies addressed the general fertility status (Brahy et al., 2000) and erodibility (Govers, 1991) of this soil material covering an undulating Tertiary landscape. Limited attention has been given to the within-field soil variability because loess soils are considered to be very homogeneous. Yet, Reyniers et al. (2006) observed important within-field variations in crop yield as a result of soil and landscape variability. However, they used only a one-year observation of crop yield. Although yield maps have been strongly promoted as a measure of crop productivity guiding the delineation of management zones for precision agriculture (Jaynes et al., 2005; Whelan et al., 2002), they often display a large temporal variation due to varying weather conditions, uneven management practices and influences of pest and diseases. To account for these variations, Lamb et al. (1997) and Boydell and McBratney (2002) suggested that more than five years of yield data are required to identify stable management zones.

Traditional general purpose soil maps, typically drawn on a scale between 1:20,000 and 1:200,000, were made for regional land use planning and are therefore not suitable to provide detailed information about the within-field variability (Robert, 1993). Soil inventory by intensive soil sampling and subsequent

* Corresponding author. Tel.: +32 9 264 5869.
E-mail address: U.Vitharana@UGent.be (U.W.A. Vitharana).

0016-7061/$ - see front matter © 2007 Elsevier B.V. All rights reserved.
doi:10.1016/j.geoderma.2007.11.003

interpolation is not a realistic alternative due to cost constraints. Thus there is a need for cost-effective, accurate and quantitative ways to explore soil information at a very detailed scale (Cook et al., 1996).

Recent advances in proximal and remote sensing and on-the-go soil and crop measurements have made available several types of ancillary information. Since these sources are capable of producing detailed spatial information, they offer a large potential to characterize the within-field soil and crop variation.

Nation-wide accurate elevation data are becoming accessible allowing the generation of digital elevation models (DEMs). From these, several terrain attributes, for example slope properties or erosion indices (Wilson and Gallant, 2000) can be obtained, which have a direct link with pedogenetic processes. Franzen et al. (2002) delineated potential management zones on the basis of topographic information, and Fraisse et al. (2001) found that management zones were closely associated with yield variation attributed to soil water availability influenced by topography.

Another widely used source of ancillary information is the measurement of soil apparent electrical conductivity (EC_a) by either electromagnetic induction or electrical resistivity measurements. Mobile EC_a measurement systems, in conjunction with a GPS, are capable of producing a large number of georeferenced data in a short period of time. One system frequently used is the electromagnetic induction sensor EM38DD (Geonics Ltd., Mississauga, ON). This sensor operates simultaneously in horizontal and vertical dipole orientations providing EC_a-H and EC_a-V measurements with investigation depths of approximately 0.75 m and 1.50 m, respectively (Hendrickx and Kachanoski, 2002). The horizontal mode receives 50% of the response from the top 0.40 m of the soil profile while similar response is achieved by the vertical mode from 0.85 m depth (McNeil, 1980). Under non-saline conditions, EC_a is mainly related to clay, water and organic matter content (Corwin and Lesch, 2005). Since these are very important properties for soil management, EC_a has been used frequently to delineate management zones (e.g. Cockx et al., 2005; Kitchen et al., 2005; Vitharana et al., 2006).

Due to the growing availability of all these information sources, and their derived products, there is a risk of over-information (Van Meirvenne, 2006). Although different ancillary information sources may reflect different levels of soil spatial variability, inter-correlations (i.e. partial duplication of information) between them are common. However, in spite of the large number of papers addressing the use of different ancillary information sources, little attention has been given to integrate such information.

This paper aims at identifying the key soil and topographic properties required to delineate potential management classes in an agricultural field in the Loess belt of Belgium. This area, having been cultivated since historical times and displays complex patterns of soil development due to the interaction of different types of soil parent material and slope processes. Data layers involved in this study were: (i) top- and subsoil textural fractions, organic carbon (OC), $CaCO_3$ (%) and pH-KCl determined at 110 locations, (ii) EC_a-V and EC_a-H measurements obtained by an EM38DD sensor and (iii) a highly accurate and detailed DEM from which several topographic attributes were calculated. The crop productivity trends across potential management classes were investigated using a three years sequence of grain and straw yield data.

2. Materials and methods

2.1. Study field

The investigated field was an 8 ha parcel located in Leefdaal (50°50′40″ N, 4°36′35″ E), Flanders, Belgium. It is situated centrally in the Belgian Loess belt, which is a part of the larger European loess area. The loess parent material is a Pleistocene aeolian sediment which originally had a thickness ranging between a few decimetres to approximately 10 m, deposited over an undulating Tertiary sandy or clayey substrate. Initially, the loess was rich in $CaCO_3$ (10–20%), But, as a consequence of the marine climate, the topsoil has decalcified down to several meters in the uneroded areas. This acidification resulted in an eluviation of clay particles creating the typical horizon sequence of loess soils of Belgium: an acidic and clay eluviated A, a clay illuviated Bt, a decalcified C1, a $CaCO_3$ containing C2 and the underlying Tertiary substrate 2C (mostly having a sandy or clayey composition). Because of the high erodibility of the loess-derived silty soil, the topography plays a significant role in soil development through erosion and deposition (Desmet and Govers, 1995). On the slopes, most of the loess, or all of it, may be eroded, while in valley bottoms colluvial deposits with a mixed composition are found.

The availability of multiple-year yield data (yield mapping is not yet a standard practise in Belgian agriculture) and the growing interest on the feasibility of adopting precision agriculture in this agriculturally important area, were the main reasons to select the study field. Moreover it displays an undulating topography, which is common for most parts of the European loess area. The field has been under a winter wheat (*Triticum aestivum*), barley (*Hordeum vulgare*) and sugar beet (*Beta vulgaris*) rotation for many years using conventional rain fed and uniform management practices. Generally soils in this area are classified as Typic Hapludalfs (Soil Survey Staff, 1982).

2.2. DEM generation and topographic attributes calculation

Elevation data collected by airborne laser scanning (LiDAR) (OC-GIS Vlaanderen, 2003) was used in this study. These data have a measurement density of approximately one point measurement per each 16–20 m^2 ground area and are characterized by very small average horizontal and vertical measurement errors (0.14 and 0.20 m, respectively). Elevation data were interpolated to a 5 m grid using punctual ordinary kriging (Goovaerts, 1997) to generate the DEM. The smallest catchment area (drainage basin) enveloping the study field was delineated using the algorithm of Jenson and Domingue (1988). Its DEM (Fig. 1a) showed that the major flow line (thalweg) of the catchment runs through the field which is located near the catchment outlet. The field consists of two plateau areas (in the east and west, the latter being the largest) gently sloping into the narrow valley floor of the thalweg (Fig. 1b). A topographic discontinuity of almost 2 m high crosses the field over

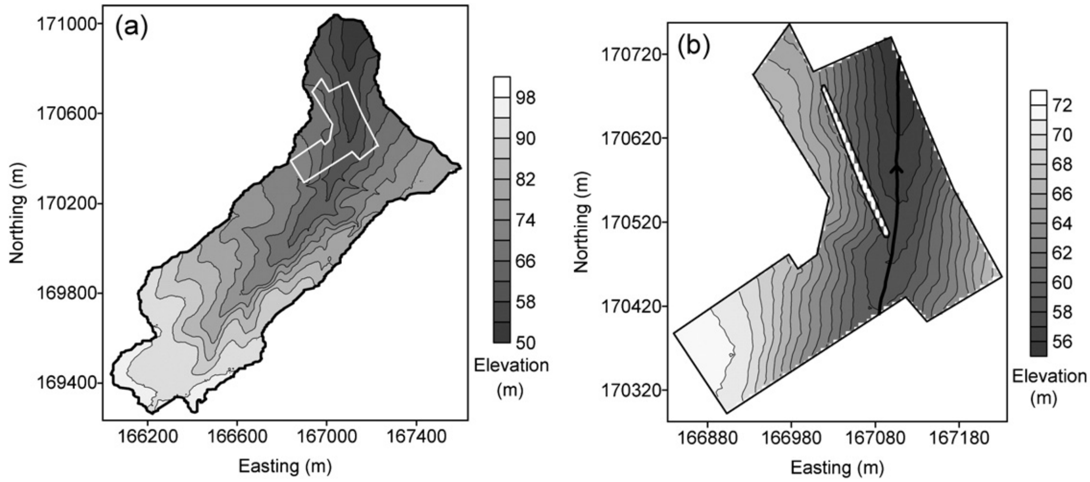

Fig. 1. (a) DEM of the smallest catchment enveloping the study field and (b) DEM of the study field indicated with the major drainage line; the topographic discontinuity is shown inside the study field.

200 m, most likely the remnant of a former hedge that might have reduced erosion locally.

Topographic attributes were calculated from the DEM using Idrisi (Kilimanjaro version, Clark Labs, Worcester, MA). The steepest slope angle (β, in degrees) and the contributing catchment area (A_s, in $m^2\ m^{-1}$) were derived on a pixel basis. The influence of the topographic discontinuity on runoff pattern was modelled by defining a height barrier along the discontinuity. Subsequently, the following secondary topographic attributes were calculated (Wilson and Gallant, 2000):

- wetness index $WI = \ln(A_s/\tan\beta)$, which is capable of predicting zones of soil water saturation (small slopes and large contributing area);
- stream power index $SPI = (A_s \times \tan\beta)$, which is a measure of the erosive power of flowing water combining the effect of upstream area and slope angle.

2.3. Soil sampling and EC_a measurements

In November 2004, soil samples were taken at 110 locations at two depth intervals (0–30 cm and 50–80 cm). Half of the sample locations were located on the nodes of a 40 m regular grid and the other half were located as a random pair associated to each grid node. At each location a pooled sample was obtained from 3 augerings within a 1 m radius. All sampling locations were georeferenced using a global positioning system (GPS) receiver with a positional accuracy of 2 to 3 m and converted into the Belgium national coordinate system (Lambert72). Air dried samples were sieved through a 2 mm sieve and analyzed for a range of agronomically important stable soil properties closely linked with the pedogenesis of loess-derived soils. These included OC (%) (by conventional Walkley and Black method), pH (in a 1 N KCl solution), $CaCO_3$ (%) and textural fractions (by pipette-sieve method).

The soil EC_a ($mS\ m^{-1}$) was measured using a dual dipole EM38DD sensor. This was connected to a field computer coupled with the GPS receiver and towed at ground level using an all terrain vehicle at a speed of about 15 km h^{-1} along 5 m spaced transects. In this way, georeferenced EC_a measurements were recorded on-the-go at 1 Hz yielding an approximate measurement density of one observation per 20 m^2.

Soil properties and EC_a measurements were geostatistically analysed. Therefore experimental variograms (omnidirectional in the absence of anisotropy, else directional) were computed and theoretical models were fit to them. Interpolation to a 5 m grid was performed with punctual ordinary kriging.

2.4. Principal component analysis (PCA) and classification into potential management classes

The 110 top and subsoil properties and their co-located EC_a and topographic attributes extracted from interpolated maps were subjected to a PCA to identify the key variables. A correlation matrix was used to equally weight all variables. To avoid the spurious correlations due to the compositional nature of the textural fractions (individual elements sum to 100%), only the clay fraction was used as an input. The strength of inter-correlations between variables was tested by the Bartlett's test of sphericity. The Kaiser–Meyer–Olkin (KMO) measure of sampling adequacy was evaluated to ensure the applicability of the data set for a PCA. A high KMO (between 0.5 and 1) is recommended. The selection of the number of retained PC's was based on the analysis of the explained variances by each PC represented by a screeplot (Cattell, 1966). To improve the interpretation of the retained PC's, a varimax rotation was applied. Finally, for each of the retained components, a representative key variable was identified based on the factor loadings. All these calculations were performed using SPSS (v. 12.0, SPSS Inc., Chicago, IL).

Kriged maps of the selected variables were classified into potential management classes using a fuzzy *k*-means classification procedure (Bezdek, 1981). This method produces a continuous grouping of objects by assigning partial class membership values, which is to be preferred for grouping properties in the soil continuum (Odeh et al., 1992). The fuzzy *k*-means classification determines the membership values for objects on the basis of minimizing the objective function $J(\mathbf{M},\mathbf{C})$. Consider a set of *n*

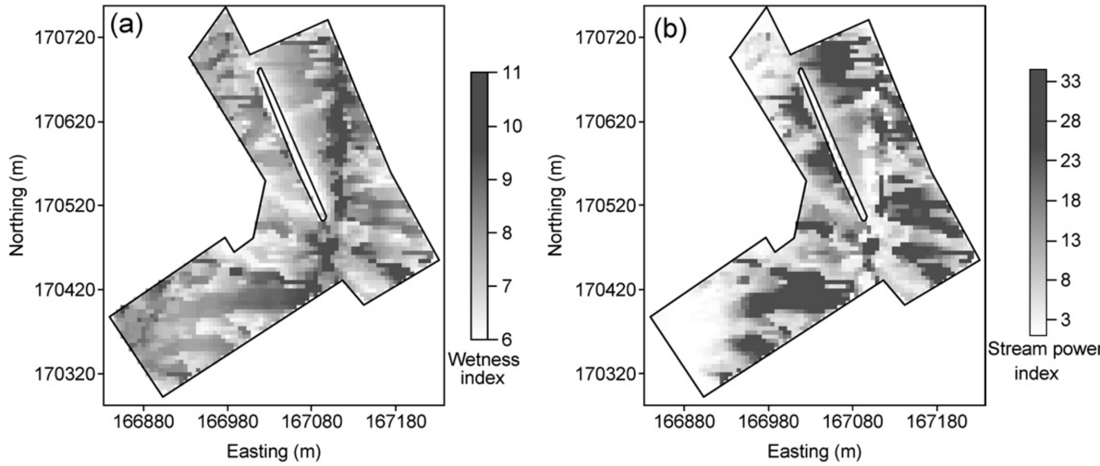

Fig. 2. Topographic attributes of the study field: (a) WI and (b) SPI.

objects (i=1,…., n) each having p attributes (v=1,…., p) grouped into k classes (c=1….., k), $J(\mathbf{M},\mathbf{C})$ can be expressed as:

$$J(\mathbf{M},\mathbf{C}) = \sum_{i=1}^{n} \sum_{c=1}^{k} m_{ic}^{\varphi} d^2(\mathbf{x}_i, \mathbf{c}_c)$$

where $\mathbf{M}=m_{ic}$ is a $n\times k$ matrix of membership values, $\mathbf{C}=c_{cv}$ is a $k\times p$ matrix of class centroids, c_{cv} denotes the centroid of class c for variable v, $\mathbf{c}_c=(c_{c1},\ldots, c_{cp})^{\mathrm{T}}$ is the vector representing the centroid of class c, $\mathbf{x}_i=(x_{i1},\ldots, x_{ip})^{\mathrm{T}}$ is the vector representing object i, $d_{ic}^{\,2}(\mathbf{x}_i,\mathbf{c}_c)$ is the square distance between $\mathbf{x}_i$ and $\mathbf{c}_c$ according to a chosen distance metric (Euclidean, Mahalanobis' or Diagonal) and φ is the fuzziness exponent which determines the degree of fuzziness of the classification (ranges between 1 and infinity, representing a crisp and a completely fuzzy classification, respectively). The fuzzy k-means classification was performed using the FuzME software (Minasny and McBratney, 2002). The fuzziness exponent was fixed to the conventional value of 1.35 (Odeh et al., 1992) and used the Mahalanobis' distance metric as it accounts for the differences in variances (Bezdek, 1981). The classification was repeated for a range of classes, i.e. k was set to a value between 2 and 8. The optimum k-value was identified on the basis of minimizing two cluster validity indices, the fuzziness performance index (FPI) and the normalized classification entropy (NCE) (Roubens, 1982). FPI ($0 \le \mathrm{FPI} \le 1$) is a measure of the degree of membership sharing among classes, where a value close to 1 indicates a strong sharing of membership and 0 represents distinct classes with no membership sharing. The NCE ($0 \le \mathrm{NCE} \le 1$) estimates the degree of disorganization in the classification and a value close to 1 indicates strong disorganization and 0 reflects superior organization.

2.5. Crop productivity among potential management classes

Yield measurements were taken during the growing seasons of 2000, 2003 (in both years winter wheat was grown) and of 2004 (barley) using the experimental grain, straw and moisture sensors of the Laboratory for Agricultural Machinery and Processing of the K.U.Leuven. The raw yield data were pre-processed to compensate for the systematic and random errors within these data (Reyniers, 2003). The data pre-processing procedure involved: removal of data with obvious positional errors, correction of measurement shifts caused by environmental factors and the noise on sensor signals and removal of irrelevant data. The grain (adjusted to a 15% reference moisture content) and straw yield maps were constructed using ordinary kriging. Generally, the spatio-temporal trend of yield is determined by averaging the yield at each grid cell over a sequence of yield maps. Since different grain crops were involved in this study, the simple averaging could not be used to investigate the yield trends across potential management classes. Therefore a standardized yield was calculated as follows (Blackmore, 1999):

$$s_{i_t} = \left(\frac{y_{i_t}}{\overline{y}_t}\right) \times 100,$$

where s_{i_t} is the standardised yield (%) at grid cell i in the year t, y_{i_t} is the interpolated yield (t ha^{-1}) and $\overline{y}_t$ is the average yield for the same year. Then, an average standardized yield map was obtained by averaging the standardized yield at each grid cell over the three years considered.

3. Results and discussion

3.1. Topographic attributes

The WI map of the field (Fig. 2a) derived from the DEM of the entire catchment (Fig. 1a) showed large values in the valley floor. Since the major flow line of the catchment passes through this valley, this area is likely to be the wettest area of the field. The rest of the field showed intermediate to small WI values. Large SPI values were found on both slopes (Fig. 2b), which resulted from the combined effect of a large upslope contribution area and a steep slope angle (on both slopes the steepest slope angle ranged between 10 and 15%), reflecting a larger tendency for surface soil loss by runoff. However, on the western slope the topographic discontinuity caused smaller SPI values on downslope since it acted as a barrier for overland water flow. Naturally, on the plateau areas the SPI values were smaller.

3.2. Soil properties

The exploratory data analysis of the soil properties (Table 1) indicated that the average texture of the topsoil and subsoil was almost identical (about 16% clay, 15% sand and 69% silt) resulting in the texture class silt loam, which is typical for soils developed in loess (Govers, 1991). However, the sand fraction showed a large variability with a coefficient of variation (CV) of 45% in the topsoil and 65% in the subsoil (ranging from 5.7 to 69.3%). The OC contents were small ranging from 0.52 to 1.01% in the topsoil (with a CV of 13%) and from 0.04 to 0.69% in the subsoil (with a much larger CV of 57%). A large variability was encountered for the pH: within this field: it ranged between 4.7 and 7.5 in the topsoil and between 4.7 and 7.7 in the subsoil. These pH differences were remarkable, since this field has been under arable land use for a long time and good agricultural practise requires this soil property to be monitored closely. Most likely only average pH values (around 6.2) were considered by the advisory institution, masking the within-field variability. Linked to the soil pH, the $CaCO_3$ content also varied largely, ranging from 0.0 to 5.8% (CV of 167%) in the topsoil and from 0.0 to 16.9% in the subsoil (CV of 189%). This was an indication of a presence of the decalcified loess and $CaCO_3$ rich loess parent material within the surface soil at different parts of the field.

Similar top- and subsoil spatial patterns were observed for all soil properties except for OC, which was quite uniform in the topsoil. Moreover, subsoil OC variability in loess landscapes is an important indication of colluvial deposits due to slope processes. It can also be beneficial to crop performance due to an improved water and nutrient holding capacity in the deeper layers.

The spatial behaviour of topsoil clay and pH and subsoil OC was investigated by modelling their omnidirectional (clay and OC) and directional (pH) variograms and these were used to produce maps by ordinary kriging. Topsoil clay (Fig. 3a) was

Table 1
Summary statistics of sampled soil properties (number of samples (n) = 110) and apparent electrical conductivity (EC_a, n = 5534)

	Mean	Minimum	Maximum	Variance	CV (%)
Topsoil					
Clay (%)	15.6	8.4	19.1	5.2	14.7
Sand (%)	15.2	8.2	46.1	46.9	45.1
Silt (%)	69.2	44.3	75.5	28.6	7.7
OC (%)	0.77	0.52	1.01	0.01	13.0
pH-KCl	6.19	4.73	7.49	0.54	11.90
$CaCO_3$ (%)	0.78	0.00	5.76	1.70	167.20
Subsoil					
Clay (%)	16.8	11.5	20.9	6.0	14.6
Sand (%)	14.3	5.7	69.3	85.2	64.5
Silt (%)	68.8	15.5	78.0	72.7	12.4
OC (%)	0.25	0.04	0.69	0.02	56.6
pH-KCl	6.23	4.69	7.72	0.71	13.50
$CaCO_3$ (%)	2.73	0.00	16.91	26.53	188.70
EC_a					
EC_a-V (mS m^{-1})	16.6	8.2	23.8	4.0	12.0
EC_a-H (mS m^{-1})	11.9	5.7	18.6	3.6	16.0

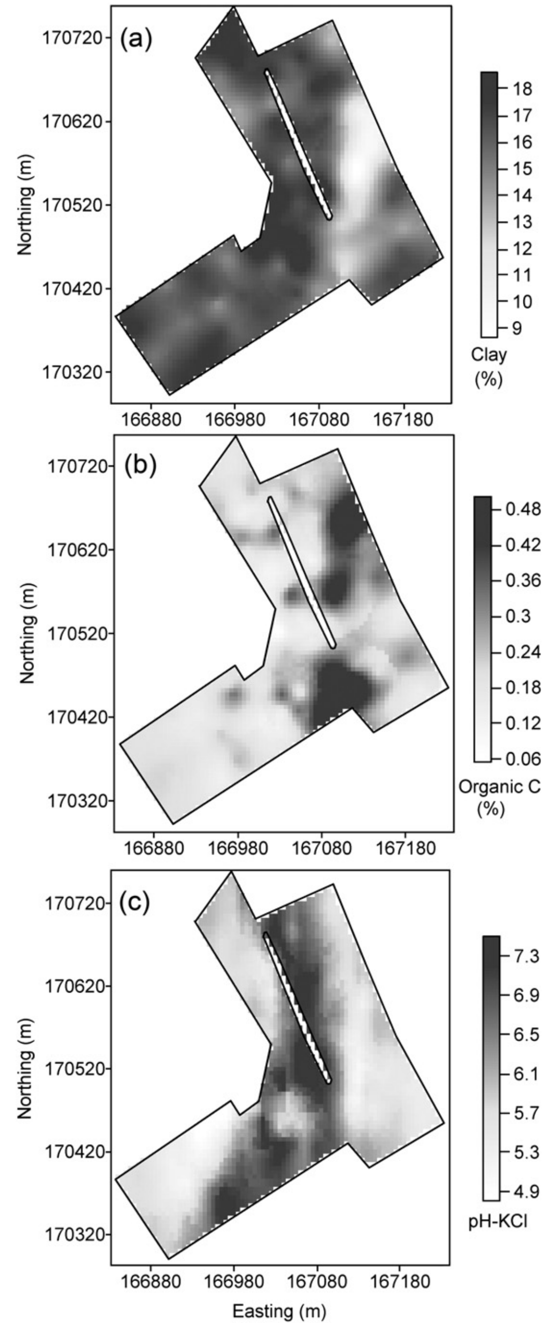

Fig. 3. Maps of kriged estimates for topsoil (a) clay content (%), (b) subsoil OC (%) and (c) topsoil pH.

uniform over most of the area, with typical values for a loess soil (15–16%). However, across the eastern slope an almost triangular area with decreased clay content (9–13%), and consequently an increased sand content, was found. The western border of this area was located next to the valley bottom (Fig. 1b) and coincided with large SPI values (Fig. 2b) resulted by the larger upslope contribution area in the S–E area of the catchment (Fig. 1a). Therefore it was likely that water erosion occurring in this part of the field might have completely removed the loess cover, exposing the underlying Tertiary sandy material (the 2C horizon). This was confirmed by the presence of surface gravel (with diameters between 0.2 and 7.5 cm) in this part of the field.

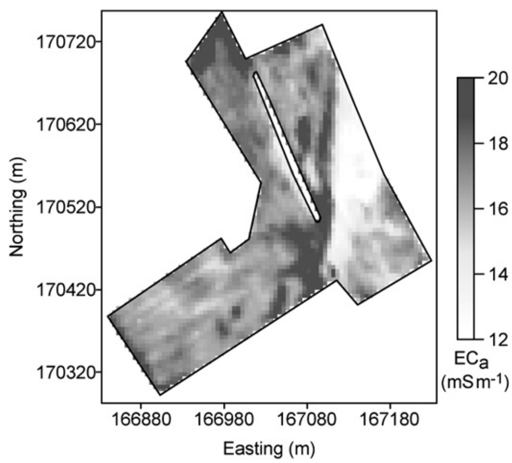

Fig. 4. Map of kriged estimates for EC_a-V.

Moreover, it is commonly observed that N–W facing slopes have a thinner loess cover due to the prevailing N–W winds during the deposition period (Pleistocene).

In most of the field the subsoil OC content was low (<0.25%) (Fig. 3b). But locally an increased level (>0.45%) was found, mainly along the valley floor. The possible cause of this was the deposition of eroded topsoil material from the slopes, together with reduced conditions for mineralization due to an increased wetness (as indicated by the WI, Fig. 2a).

The topsoil pH map (Fig. 3c) showed a N–S oriented band of higher pH values (>6.6) over the western slope, more or less parallel to the valley bottom. Within this band increased top- and subsoil $CaCO_3$ contents were found. This suggested that on this slope, the decalcified A, Bt and C1 horizons were removed, exposing the $CaCO_3$ rich loess parent material (C2 horizon). This indicated less severe erosive conditions than on the eastern slope, where all loess material was removed. The past presence of a hedge, which has resulted in the topographic discontinuity, might have reduced the erosive power on this slope, as reflected by the reduced SPI-values. Additionally, S-E facing slopes originally were covered by thicker loess layers. The rest of the field generally showed a lower pH (<5.8), with no $CaCO_3$ in topsoil or subsoil. This variability obviously has important implications for lime applications, which is a routine practice by farmers in this area. Some areas within this field (the plateau areas and the eastern slope) require liming, whereas the western slope does not.

3.3. Apparent electrical conductivity

Table 1 shows the descriptive statistics of the measured EC_a values. The average EC_a-V was 16.6 mS m^{-1} while the average EC_a-H was 11.9 mS m^{-1}. The lower values of EC_a-H indicated a lower topsoil conductivity which might have been the result of the somewhat drier topsoil, compared to the subsoil. Both variables had a similar variance and similar CV's (12% for EC_a-V and 16% for EC_a-H), which indicated a moderate level of variability, compared to most of the soil properties. A strong correlation ($r=0.90$) was found between EC_a-V and EC_a-H with similar variograms and interpolated maps. Therefore the kriged map of EC_a-V is shown in Fig. 4. This map shows that EC_a-V was low on the eastern slope (<14.5 mS m^{-1}), a pattern mainly observed on the topsoil clay (Fig. 3a) and sand map. This was confirmed by the rather strong correlation between EC_a-V and topsoil clay ($r=0.7$) and sand ($r=-0.7$). A number of studies (e.g. Corwin and Lesch, 2005; Vitharana et al., 2006) reported similar relationships between EC_a and soil textural fractions. The valley floor was distinct on the EC_a map, with large values (>18.5 mS m^{-1}) reflecting the wetter soil conditions and the increased OC content in the subsoil. The rest of the field was fairly homogeneous with moderate EC_a values.

3.4. Principal component analysis

The Bartlett's test of sphericity indicated a significant correlation between the variables since the correlation matrix was statistically different from an identity matrix ($\chi^2=1192.5$, $p<0.05$). The KMO measure was 0.67 indicating that the sampling was adequate for PCA. Based on a screeplot of the eigenvalues the first 3 PC's were retained, which accounted for 67.4% of the total variance. Table 2 gives the communalities and loadings of the variables on the 3 rotated PC's. The smallest communality was 0.23, but most were larger than 0.6. This showed that the three retained PC's explained most of the variance in the original dataset.

Fig. 5 provides the loading plots. The first PC (reflecting 30.5% of the total variance) was strongly associated with top- and subsoil pH and $CaCO_3$ content, with subsoil pH having the largest loading on PC1 (0.872). Also the slope angle showed a strong association with this PC. The second PC covered 21.3% of the total variance and had the strongest contribution from the two EC_a variables (the largest loading on PC2 was for EC_a-V: 0.927) and top- and subsoil clay content. The third component

Table 2
Factor loading of the rotated first three PC's with labels (inside parenthesis) used in Fig. 5

Variable and label identification	Communality of first 3 PC's	Principal component loadings		
		PC1	PC2	PC3
Topsoil				
OC (1)	0.50	0.045	0.047	0.700
pH (2)	0.85	0.818	0.307	0.300
$CaCO_3$ (3)	0.67	0.814	0.058	−0.043
Clay (4)	0.83	0.312	0.826	−0.219
Subsoil				
OC (5)	0.67	−0.308	−0.254	0.707
pH (6)	0.83	0.872	0.083	0.255
$CaCO_3$ (7)	0.71	0.837	−0.015	−0.098
Clay (8)	0.64	−0.174	0.641	−0.448
EC_a and topographic attributes				
EC_a-V (9)	0.90	0.064	0.927	0.173
EC_a-H (10)	0.90	0.153	0.923	0.152
Elevation (11)	0.66	−0.232	0.456	−0.627
Slope (12)	0.56	0.718	0.038	−0.202
WI (13)	0.51	−0.382	0.051	0.604
SPI (14)	0.23	0.137	0.100	0.446

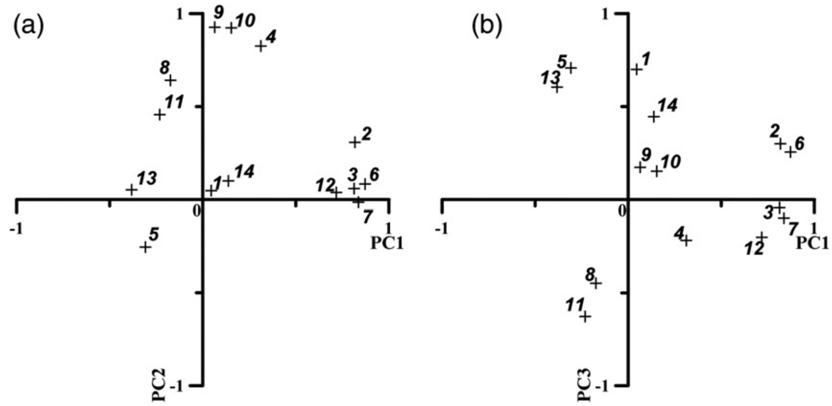

Fig. 5. Rotated loading plots of the (a) first and second PC and (b) first and third PC. Label identifications and loading values are given in Table 2.

accounted for 15.6% of the total variance and represented mainly top- and subsoil OC (the largest loading on PC3 was for subsoil OC: 0.707), elevation and the WI. SPI was weakly associated to any of these three PC's and appeared to be less informative.

The PCA results suggested an independent spatial behaviour along three major factors, dominated by pH, EC_a and OC respectively. Currently, intensive observations of EC_a-V and pH can be obtained by commercially available on-the-go sensors (Adamchuk et al., 2005). On-the-go sensors suitable for OC determinations (e.g. NIR sensor) are just becoming operational in practise. Therefore, elevation was selected as an easy-to-obtain surrogate for OC, since it had the second largest loading on PC3 after top- and subsoil OC. However, Moore et al. (1993) observed a strong association between OC and WI in a different landscape setting.

3.5. Potential management classes delineation

As a result from the PCA, topsoil pH, EC_a-V and elevation were used as input variables to the fuzzy *k*-means classification. FPI and NCE were minimized for four classes, i.e. $k=4$. The map of the potential management classes (Fig. 6a) was obtained by a generalization of the fuzzy *k*-means class membership map by removing a few small island clusters which were not feasible for practical site-specific management purposes. A clear link between these management classes and the landscape position was recognized using a cross-section of elevation across classes (Fig. 6b).

Class 1 occupied the southwest, northwest and southeast parts of the field and covered the largest area. Three zones of this class covered the highest plateau and upslope positions of the field, i.e. the areas least modified by slope processes. In this class the typical A-Bt-C1-C2-2C acidic silt loam soil of the loess area was found. This was confirmed by the average soil properties of the samples located inside this class (Table 3). The average soil properties of class 1 were therefore used as a reference to compare the properties of the other classes.

Class 2 coincided with the less eroded western slope where the $CaCO_3$ rich loess parent material was exposed (C2 layer), partially limited by the topographic discontinuity. Soil texture was similar to class 1, but class 2 had an increase in pH and $CaCO_3$ content (Table 3).

Class 3 covered the severely eroded eastern slope, exposing partially the 2C sandy substrate. Due to the tillage activities, this

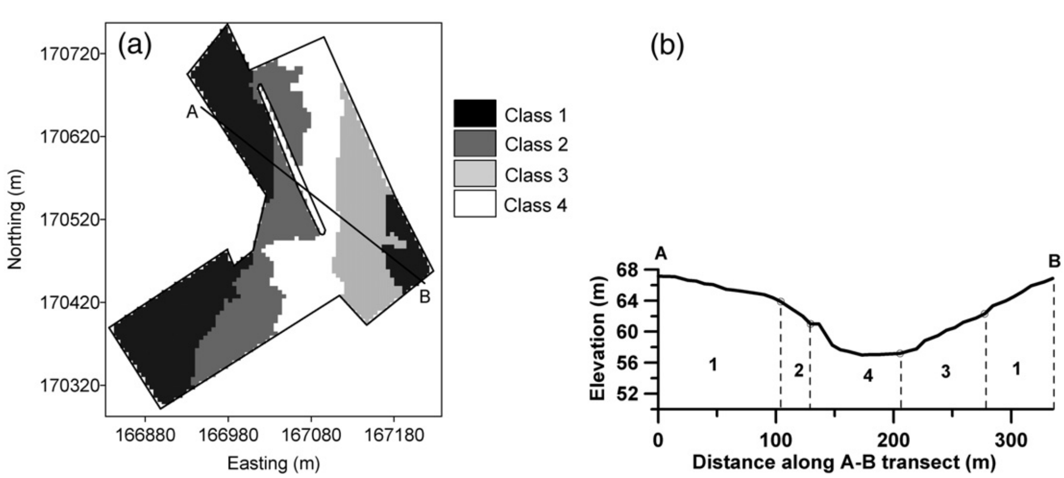

Fig. 6. (a) Potential management classes delineated using topsoil pH, EC_a-V and elevation. (b) elevation along A–B with indication of the potential management classes.

Table 3
Mean values of soil properties and yield data for each potential management class (with standard deviations between brackets)

	Mean			
	Class 1	Class 2	Class 3	Class 4
Topsoil				
Clay (%)	16.2 (1.3)	16.8 (0.9)	12.5 (2.9)	15.0 (2.1)
Silt (%)	70.7 (1.8)	71.1 (1.9)	62.6 (9.5)	69.4 (3.3)
Sand (%)	13.0 (2.1)	12.0 (2.1)	24.7 (11.4)	15.5 (3.5)
pH	5.6 (0.4)	7.0 (0.4)	5.5 (0.4)	6.2 (0.5)
OC (%)	0.72 (0.08)	0.78 (0.12)	0.76 (0.09)	0.83 (0.12)
$CaCO_3$ (%)	0.16 (0.14)	1.90 (1.87)	0.30 (0.20)	0.38 (0.16)
Subsoil				
Clay (%)	18.7 (1.2)	16.8 (1.7)	14.7 (2.8)	15.7 (2.6)
Silt (%)	70.0 (2.0)	72.4 (3.2)	59.2 (16.7)	69.7 (2.7)
Sand (%)	11.3 (1.8)	10.8 (3.1)	26.1 (16.9)	14.7 (4.3)
pH	5.5 (0.5)	7.1 (0.5)	5.9 (0.6)	6.1 (0.4)
OC (%)	0.2 (0.06)	0.19 (0.07)	0.27 (0.12)	0.4 (0.15)
$CaCO_3$ (%)	0.22 (0.27)	7.41 (6.81)	0.74 (1.25)	0.35 (0.24)
Three-year average standardized yield				
Grain (%)	95.7 (7.1)	99.4 (8.5)	103.7 (7.6)	104.7 (7.7)
Straw (%)	94.4 (9.3)	98.7 (11.1)	102.9 (11.6)	108.2 (11.7)

sand was mixed with the remaining silt loam causing the average sand content to double compared to class 1, but pH and OC remained similar (Table 3).

Class 4 represented the valley floor. Texture, pH and $CaCO_3$ were quite similar to class 1, but the OC content was increased, especially in the subsoil (Table 3).

3.6. Crop productivity and potential management classes

The three-year average standardized yield maps of grain and straw (%) are shown in Fig. 7a and b. Visually, no strong relationship could be observed for the grain yield, but for straw there was a better correspondence with the management classes. In particular, class 4 (the valley floor) had an average higher straw productivity.

The three-year average standardized grain and straw yield was split per class and the result is given in Table 3. Straw was more variable than grain. The highest productivity occurred in class 4: 104.7% for grain and 108.2% for straw. The lowest yield was found in class 1: the plateau and upslope areas. Classes 2 and 3 had intermediate values, with class 3 slightly above average and class 2 slightly below average. The sandy substrate of class 3 did not result in a yield decline in the three years considered. The relatively clay rich class 1 produced lower yields, indicating that during those years, crop productivity did not fully reflect the general soil fertility variation of the studied field. However the yield trends represented to some degree the delineated management classes in relation to the landscape position (Fig. 6b). Therefore, in the three years considered, crop productivity was likely driven by variations in moisture availability related to the landscape position. Weather records of the three considered growing seasons indicated that average (2000) to rather dry weather conditions (2003 and 2004) prevailed. So the crop might have benefited from the wetter conditions in the valley floor and the reverse on the higher landscape positions. However, it should be realized that in dominantly wet climatic conditions this relationship might invert. In the case of an extreme rain event, a temporary flooding or fully saturated conditions might even destroy completely the crop in the valley floor. So crop production in the valley floor is likely to be more variable between years than in the other classes. Kaspar et al. (2003) and Reuter et al. (2005) made similar observations by investigating the relationships between landform units and yield potential.

4. Conclusions

A strongly structured spatial variation of several soil properties at a within-field scale in a loess-derived soil with undulating topography was found. Although overall soil texture was a homogeneous silt loam, on the eastern slope soil texture was sandier, OC increased in the subsoil of the valley bottom and $CaCO_3$ and pH were much higher along a band on the western slope. These patterns originated most likely from different levels of soil erosion. These differences support the implementation of differential soil management practices at a field scale.

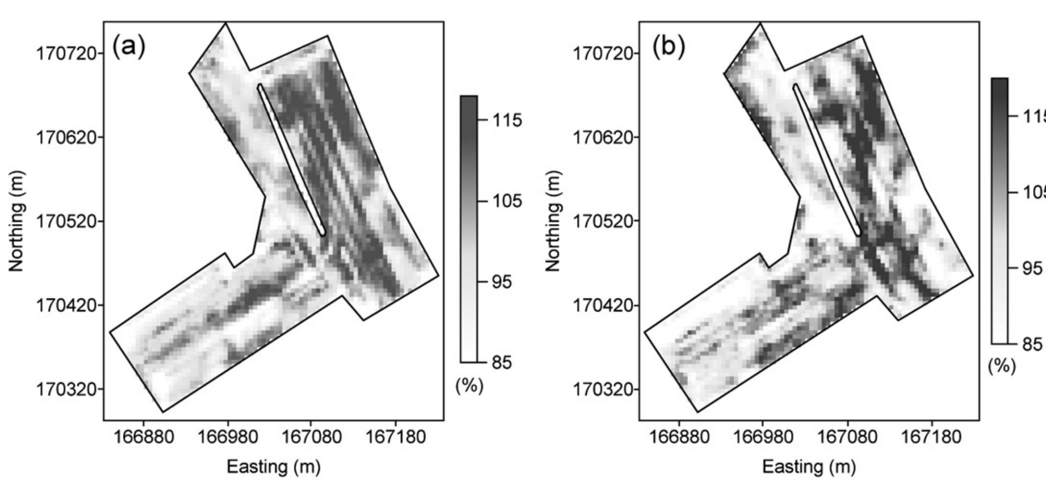

Fig. 7. Three-year average standardized yield map of (a) grain and (b) straw.

A PCA highlighted the importance of pH, EC_a-V (as a surrogate for soil texture) and OC as independent key variables to characterise the overall soil variation. Since on-the-go sensors for OC are just becoming operational, OC was replaced by elevation, the second most dominant variable on the principal component associated with OC variation. In this way all three key properties could be obtained without intensive soil sampling and costly laboratory analyses.

These three key variables were used to identify and delineate four classes using a fuzzy *k*-means algorithm. Clear differences in top- and subsoil properties and landscape position were found between these classes and also the three-year average standardised grain and straw yields were different across the classes. The yield differences were more related to differences in topography across classes and less to the spatial variability of soil properties.

The results indicated that the variability of pH, texture and OC was suitable to delineate potential management classes. Since similar pedogenetic processes occurred in most parts of the undulating European loess landscape, it can be expected that these findings can be extended to a broader scale.

It was concluded that in the loess area, with complex soil-landscape interactions, pH, EC_a and elevation can be defined as the key properties to delineate potential management classes for precision agriculture.

Acknowledgements

Udayakantha W.A. Vitharana thanks the Ghent University for providing financial support under the special research fund (BOF) to carry out this study. The authors thank Dr. Mieke Reyniers of Flemish land agency for providing pre-processed yield data. They also acknowledge Mathieu Schatteman and Luc Deboosere of the Department of Soil Management and Soil Care for their support in the field and laboratory work.

References

Adamchuk, V.I., Lund, E.D., Sethuramasamyraja, B., Morgan, M.T., Dobermann, A., Marx, D.B., 2005. Direct measurement of soil chemical properties on-the-go using ion-selective electrodes. Computers and Electronics in Agriculture 48 (3), 272–294.

Bezdek, J.C., 1981. Pattern Recognition with Fuzzy Objective Function Algorithms. Premium Press, New York, NY.

Blackmore, S., 1999. The interpretation of trends from multiple year maps. Computers and Electronics in Agriculture 26 (1), 37–51.

Boydell, B., McBratney, A.B., 2002. Identifying potential within-field management zones from cotton-yield estimates. Precision Agriculture 3 (1), 9–23.

Brahy, V., Deckers, J., Delvaux, B., 2000. Estimation of soil weathering stage and acid neutralizing capacity in a toposequence Luvisol–Cambisol on loess under deciduous forest in Belgium. European Journal of Soil Science 51, 1–13.

Cattell, R.G., 1966. The scree test for the number of factors. Multivariate Behavioral Research 1, 245–276.

Cockx, L., Van, n Meirvenne, M., Hofman, G., 2005. Characterization of nitrogen dynamics in a pasture soil by electromagnetic induction. Biology and Fertility of Soils 42, 24–30.

Cook, S.E., Corner, R.J., Grealish, G., Gessler, P.E., Chartres, C.J., 1996. A rule-based system to map soil properties. Soil Science Society of America Journal 60, 1893–1900.

Corwin, D.L., Lesch, S.M., 2005. Characterizing soil spatial variability with apparent soil electrical conductivity: I. survey protocols. Computers and Electronics in Agriculture 46, 103–133.

Desmet, P.J.J., Govers, G., 1995. GIS-based simulation of erosion and deposition patterns in an agricultural landscape: a comparison of model results with soil map information. Catena 25, 389–401.

Franzen, D.W., Hopkins, D.H., Sweeney, M.D., Ulmer, M.K., Halvorson, A.D., 2002. Evaluation of soil survey scale for zone development of site-specific nitrogen management. Agronomy Journal 94, 381–389.

Fraisse, C.W., Sudduth, K.A., Kitchen, N.R., 2001. Delineation of site-specific management zones by unsupervised classification of topographic attributes and soil electrical conductivity. Transactions of the ASAE 44 (1), 155–166.

Goovaerts, P., 1997. Geostatistics for Natural Resource Evaluation. Oxford University Press, New York, NY.

Govers, G., 1991. Rill erosion on arable land in central Belgium: rates, controls and predictability. Catena 18 (2), 133–155.

Hendrickx, J.M.H., Kachanoski, R.G., 2002. Indirect measurement of solute concentration: Nonintrusive electromagnetic induction. In: Dane, J.H., Topp, G.C. (Eds.), Methods of soil analysis. SSSA Book, Ser. 5 Part 4. SSSA, Madison, WI, pp. 1297–1306.

Jaynes, D.B., Colvin, T.S., Kaspar, T.C., 2005. Identifying potential soybean management zones from multi-year yield data. Computers and Electronics in Agriculture 46, 309–327.

Jenson, S.K., Domingue, J.O., 1988. Extracting topographic structure from digital elevation data for geographic information system analysis. Photogrammetric Engineering and Remote Sensing 54, 1593–1600.

Kaspar, T.C., Colvin, T.S., Jaynes, D.B., Karlen, D.L., James, D.E., Meek, D.W., Pulido, D., Buttler, H., 2003. Relationship between six years of corn yields and terrain attributes. Precision Agriculture 4 (1), 87–101.

Kitchen, N.R., Sudduth, K.A., Myers, D.B., Drummond, S.T., Hong, S.Y., 2005. Delineating productivity zones on claypan soil fields using apparent soil electrical conductivity. Computers and Electronics in Agriculture 46, 285–308.

Lamb, J.A., Dowdy, R.H., Anderson, J.L., Rehm, G.W., 1997. Spatial and temporal stability of corn grain yields. Journal of Production Agriculture 10, 410–414.

McNeil, J.D., 1980. Electromagnetic Terrain Conductivity Measurement at Low Induction Numbers: Technical Note TN-6. GEONICS Limited, Ontario.

Minasny, B., McBratney, A.B., 2002. FuzME Version 3, Australian Centre for Precision Agriculture, The University of Sydney, NSW 2006.

Moore, I.D., Gessler, P.E., Nielsen, G.A., Peterson, G.A., 1993. Soil attribute prediction using terrain analysis. Soil Science Society of America Journal 57, 443–452.

OC-GIS Vlaanderen, 2003. Digitaal Hoogtemodel Vlaanderen. Nieuwsbrief GIS-Vlaanderen, 16. VLM, Brussel (in Dutch).

Odeh, I.O.A., McBratney, A.B., Chittleborough, D.J., 1992. Soil pattern recognition with fuzzy-c-means: application to classification and soil–landform interrelationships. Soil Science Society of America Journal 56, 505–516.

Reyniers, M., 2003. Precision farming techniques to support grain crop production. Ph.D. Dissertation. Katholieke Universiteit Leuven. Faculty of Agricultural and Applied Biological Sciences, pp. 47–52.

Reyniers, M., Maertens, K., Vrindts, E., De Baerdemaeker, J., 2006. Yield variability related to landscape properties of a loamy soil in central Belgium. Soil & Tillage Research 88, 262–273.

Reuter, H.I., Giebel, A., Wendroth, O., 2005. Can landform stratification improve our understanding of crop yield variability? Precision Agriculture 6 (6), 521–537.

Robert, P., 1993. Characterization of soil conditions at the field level for soil specific management. Geoderma 60, 57–72.

Roubens, M., 1982. Fuzzy clustering algorithms and their cluster validity. European Journal of Operational Research 10, 294–301.

Soil Survey Staff, 1982. Soil taxonomy. Agricultural Handbook, 436. Soil Conservation Service, USDA, Washington, DC (with amendments).

Van Meirvenne, M., 2006. Soil inventory in transition: from too few to too many geo-data? In: Hartemink, A. (Ed.), The Future of Soil Science. IUSS, Wageningen, pp. 142–144.

Vitharana, U.W.A., Van Meirvenne, M., Cockx, L., Bourgeois, J., 2006. Identifying potential management zones in a layered soil using several sources of ancillary information. Soil Use and Management 22, 405–413.
Whelan, B.M., Cupitt, J., McBratney, A.B., 2002. Practical definition and interpretation of potential management zones in Australian dryland cropping. In: Robert, P.C., Rust, R.H., Larson, W.E. (Eds.), Precision Agriculture. ASA-CSSA-SSSA, Madison, WI, pp. 325–329.
Wilson, J.P., Gallant, J.C., 2000. Terrain Analysis: Principals and Applications. John Wiley & Sons, New York, NY.